24th INTERNATIONAL CONGRESS ON SOUND AND VIBRATION
23–27 July 2017, London

ICSV24
23-27JULY 2017
LONDON CALLING

USE OF FLAME TRANSFER FUNCTION TO PREDICT COMBUSTOR UNSTABLE MODES

Ennio Luciano, Eduardo Tizné and Javier Ballester

Laboratory for Research on Fluid Dynamics and Combustion Technologies (LIFTEC), CSIC - University of Zaragoza, María de Luna 10, 50018 Zaragoza, Spain
email: eluciano@liftec.unizar-csic.es

The use of low-order network models to predict the natural modes of a burner is a very useful tool especially during the early stage of combustor design. In particular, the prediction of the unstable modes, which can generate limit cycle conditions, is a major objective of these simulations. A few studies have shown that the flame transfer function (FTF), i.e. linear flame response, can also be used to predict unstable, non-linear modes, both in their frequency and in their growth rate. In order to further assess the validity of this approach, predictions with this simplified method have been compared with experimental results for a broad range of conditions, in most cases reaching limit cycle regimes. Two different fuels, methane and biogas, have been studied for two different burner lengths and varying both the equivalence ratio and the upstream reflection coefficient. The results of the model coincide quite well in their real part with the experimental frequencies measured, while the imaginary part of the solution reveals the instability of the modes obtained. So, the results validate the viability of this approach for a broad range of operational conditions, including the differences in dynamic flame response between methane and biogas.

Keywords: Flame Dynamics, Dispersion Equation, Limit Cycle, Flame Transfer Function

1. Introduction

Lean premixed combustion has become the leading technology in gas turbines field because of its high efficiency combined with very low pollutant emissions [1]. However, combustion dynamics has risen as a major problem since lean combustion has shown proneness to the coupling of flame heat flux fluctuation (Q') with pressure oscillations in the combustion chamber (p').

According to Rayleigh's criterion [2], the in-phase oscillation of these two magnitudes, if their product is greater than irreversible losses, produces a strong increment of p' fluctuation, eventually reaching limit cycle conditions, which can cause serious damages to the hardware.

Prediction of instability modes is an important objective, especially at the early stage of combustor design. Two main approaches can be followed [3]: on the one hand, the direct calculation of both acoustic waves and unsteady heat release through CFD simulations is a possibility, even if really onerous at computational level. On the other hand, the development of simplified network models, in which burner elements are modelled using linear acoustics (in terms of transfer or scattering matrices) and, then, are connected in series, has shown a high potential to identify unstable ranges.

Previous works suggest that linear acoustics correctly describes the behaviour of the system, except for the flame response [3, 4].Therefore, an accurate model of non-linear flame dynamics combined with simple transfer matrices of the other elements may provide good predictions of the unstable modes of the system studied.

In this context, many authors have performed simulations combining linear models of the burner elements and non-linear flame dynamics (e.g., [3-6]), which can be resumed by a family of curves called flame describing function (FDF). Nevertheless, some studies successfully used the flame transfer function (FTF), i.e. the linear flame response, for the prediction of natural unstable modes [7-10]. The use of FTF, instead of FDF, as an input to the model significantly simplifies the procedure to describe the dynamic response of the flame and, so, it reduces the effort and time required to predict combustor stability. The results obtained in previous works are encouraging, and the objective here is to explore in a systematic way a relatively wide range of operational conditions, including fuel composition, in order to evaluate the feasibility of predicting unstable modes based on simplified descriptions of the system and, especially, of the flame response.

In this work, a simplified model, called *dispersion equation*, has been used to predict unstable modes of a lab-scale, gas turbine burner using FTF as an input. A wide range of possible situations has been explored, which includes variations in geometry (burner length, upstream reflection coefficient), equivalence ratio and fuel composition. In particular, a specific objective was to evaluate the ability of the model and of the FTF to successfully capture the impact of changes in fuel properties on combustor stability. With this aim, the experimental results for both methane and biogas flames have been compared with the predictions of the model. The formulation of the dispersion equation is developed in Section 2, while Section 3 describes the experimental rig as well as experiments performed and instrumentation used. Section 4 is dedicated to the results discussion, and the main conclusions are summarized in Section 5.

2. Dispersion equation

Figure 1 shows a simplified scheme of the burner used for the experiments, which will be used as a reference to develop the model. Further details are given in Section 3. This combustion rig can be modelled as a two-cavity system and, for the frequencies of interest, the flame can be considered compact. Therefore, the low-order network model of the entire system can be reduced to a single equation, called *dispersion equation*. The main steps which lead to the final formulation of the model are outlined in this section; for a more in-depth analysis, references [7, 11, 12] are recommended.

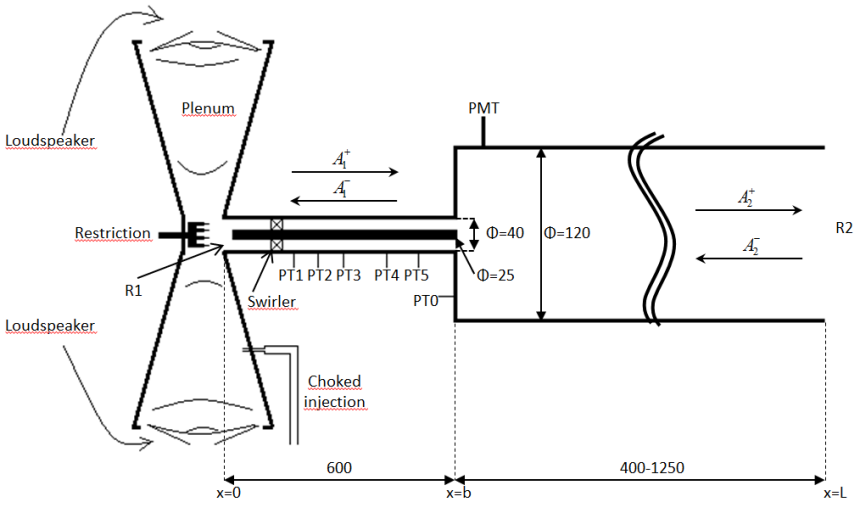

Figure 1. Scheme of the burner (all dimensions in mm).

$A_{1,2}^{+,-}$ represents plane waves travelling forward (+)/backward (-) inside the injection duct (1) and combustion chamber (2). The same notation will be used from now on to designate variables in both sections (1, 2) and propagation directions (+, -). Supposing small values of Mach number and constant mean pressure (p) and specific heat ratio (γ) in both elements, according to linear acoustic theory pressure fluctuation is conserved at the discontinuity ($x=b$), while there is a sudden jump in velocity oscillation, dependent on the area (S) variation and on the fluctuation of heat release rate, Q'

(the flame is assumed to be located very close to the dump plane).These conditions are expressed in Eqs. (1-2), where $b_{+,-}$ indicates right (+)/left (-) handed limits, as x approaches b.

$$p'(b_-) = p'(b_+) \tag{1}$$

$$S(b_+)\cdot u'(b_+) - S(b_-)\cdot u'(b_-) = \frac{\gamma-1}{\gamma\cdot p}Q' \tag{2}$$

Assuming a harmonic variation of both acoustic variables and heat release rate, continuity conditions can be reformulated as in Eqs. (3-4), where ρ and c represent the mean density and the speed of sound, respectively. k is the wave number, defined as $k^{\pm} = \omega/(c \pm u)$, with ω and u designating angular frequency and mean flow velocity, respectively.

$$A_2^+ + A_2^- = A_1^+ e^{-ik_1^+ b} + A_1^- e^{ik_1^- b} \tag{3}$$

$$\frac{S_2}{\rho_2 c_2}(A_2^+ - A_2^-) = \frac{S_1}{\rho_1 c_1}(A_1^+ e^{-ik_1^+ b} - A_1^- e^{ik_1^- b}) + \frac{\gamma-1}{\gamma\cdot p}Q' \tag{4}$$

Upstream and downstream reflection coefficients (R_1 and R_2) can be defined as in Eq. (5), where L indicates the total length of the rig:

$$R_1 = \frac{A_1^+}{A_1^-}; R_2 = \frac{A_2^- e^{ik_2^-(L-b)}}{A_2^+ e^{-ik_2^+(L-b)}} \tag{5}$$

Rearranging Eq. (3) and (4), in order to make R_1, R_2 and FTF explicit, leads to the dispersion equation (Eq. (6)), which completely describes the burner acoustics:

$$\begin{aligned}&(1+\Gamma_1+\Gamma_2\cdot FTF)\cdot\left(R_1\cdot R_2\cdot e^{-i[b(k_1^+ + k_1^-)+(L-b)\cdot(k_2^+ + k_2^-)]} - 1\right) + \\ &(1-\Gamma_1-\Gamma_2\cdot FTF)\cdot\left(R_2\cdot e^{-i\cdot(L-b)\cdot(k_2^+ + k_2^-)} - R_1\cdot e^{-i\cdot b\cdot(k_1^+ + k_1^-)}\right) = 0\end{aligned} \tag{6}$$

Γ_1 and Γ_2 are two variables dependent on physical parameters and rig dimensions, as shown in Eq. (7), where Q indicates the mean heat flux.

$$\Gamma_1 = \frac{\rho_2 c_2 S_1}{\rho_1 c_1 S_2}; \Gamma_2 = \frac{\rho_2 c_2}{\rho_1 c_1 S_2}\frac{\gamma-1}{\rho_1 c_1^2}\frac{Q}{u} \tag{7}$$

Solutions of Eq. (6) in terms of ω (hidden into k values) are the natural modes of the burner. The solutions are complex numbers, whose real part indicates oscillation frequency, while the sign of the imaginary part reveals if the solution is stable ($Im(\omega)>0$) or unstable ($Im(\omega)<0$). The dispersion equation has been applied to the experimental conditions explained in the next section.

3. Experimental method

3.1 Experimental rig

Tests have been performed in an atmospheric, swirl-stabilized, premixed combustor facility consisting of a plenum, an annular duct and a combustion chamber (main dimensions as in Fig. 1). Fuel is premixed with air upstream of the plenum and injected into it through two choked orifices in order to prevent ER fluctuations. The air-fuel mixture flows into the annular duct, passing through an axial swirler (six 30º vanes) located 380 mm upstream of the dump plane. The acoustic boundary condition R_1 at the entrance of the injection duct can be modified by manipulating an adjustable restriction. As sketched in Fig. 1, this restriction is shaped as a crenelated plug, with eight, 25 mm high teeth. The relative position between the plug and the duct entrance can be adjusted. This setting will be identified by the coordinate H, expressing the length of the teeth inserted into the duct: H=0 means that the tips are aligned with the duct inlet, which is gradually restricted as H increases until completely closed for H=25 mm. H=-infinity indicates that the plug is withdrawn and the inlet is fully open.

The combustion chamber is composed of a first, optically accessible, quartz section (220 mm in length) followed by a second stainless steel one, whose length can be changed by installing different segments, so that the total chamber length can be set to 400, 900 or 1250 mm.

Five piezoelectric pressure transducers (PT1-5 in Fig. 1, PCB 103B02) are located at various positions along the annular duct, while another one (PT0) measures *p'* in the combustion chamber. Flame heat flux is determined using a photomultiplier tube (PMT, Hamamatsu H5784-03), fitted with an OH* band interference filter (310±5 nm). Two loudspeakers (10", Eminence DELTA-10A), powered by the same amplifier, are installed at both sides of the plenum to provide acoustic excitation to the premixed flow. Another loudspeaker (8", HQ Power VDSSP8/8) can be installed, in absence of flame, at the combustor exit to acoustically excite the facility from the top.

3.2 Flame and rig characterization

Apart from physical magnitudes (such as densities, speeds of sound etc.) and geometrical dimensions, some parameters involved in the dispersion equation have to be determined experimentally. In particular, FTF and reflection coefficients must be determined in ad-hoc tests, as explained in the following sub-sections.

3.2.1 Upstream reflection coefficient

The combustion chamber outlet was open to the atmosphere in all tests and, hence, the downstream reflection coefficient was taken as R_2=-1 for the calculations. Instead, R_1 value can be changed by modifying the position of the restriction and so it had to be measured. To do so, an 8" loudspeaker was located in front of the combustor outlet to provide acoustic forcing at frequencies from 50 to 600 Hz with 10 Hz step. *p'* was measured (4 s, 4 kHz) with the five PTs located along the annular duct and the multi-microphone method [13] was applied in order to determine the two Riemann invariants in the duct, and so the value of R_1. The results for different H settings are shown in Fig. 2 and were used as an input for the dispersion equation model. The tests were repeated for different combustor lengths, forcing amplitudes and air mass flows injected into the rig (from 0 to 40 Nm^3/h); however, R_1 displayed negligible differences and so it was taken as constant for all test conditions. R_1 results show similar patterns for *H* values from 0 to 20 mm in magnitude and phase, with the latter depicting an almost linear trend with frequency whose slope slightly increases with restriction level. A different behaviour is obtained for the fully open inlet (*H*=-inf), especially for the phase, which is almost constant around π, resembling the acoustic condition of an open end.

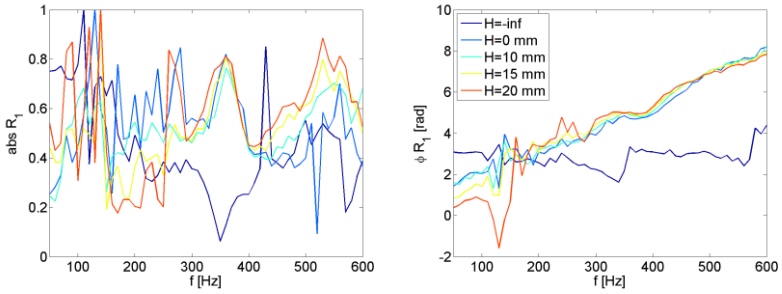

Figure 2. R_1 absolute value and phase for various restriction levels

3.2.2 FTF tests

The flame transfer function was measured for the short combustion chamber (400 mm), in order to avoid self-excited instabilities, which otherwise would strongly affect the results. Acoustic forcing was provided by the two loudspeakers located in the plenum, for the same sampling frequency, recording time and excitation frequencies described above for R_1 tests. The amplitude was regulated at sufficiently high levels to obtain meaningful results but always within the linear regime. The multi-microphone method was applied to calculate *u'* value at the dump plane, while both mean and fluctuating value of heat flux were measured with PMT. FTF tests were performed at five different ER (0.98, 0.92, 0.86, 0.80, 0.72) for two different fuels: methane and a CH_4-CO_2 blend (60-40% in

volume), representative of biogas. Methane flow rate was kept constant at 3 Nm^3/h in all tests, changing the air mass flow in order to vary ER. For biogas cases, the air-fuel mass flow was set to achieve the same ER and mean injection velocity as in CH_4 tests. As a consequence, power cannot be the same for the two fuels, however differences are really low (7% in the worst case). FTF results are shown in Fig. 3.

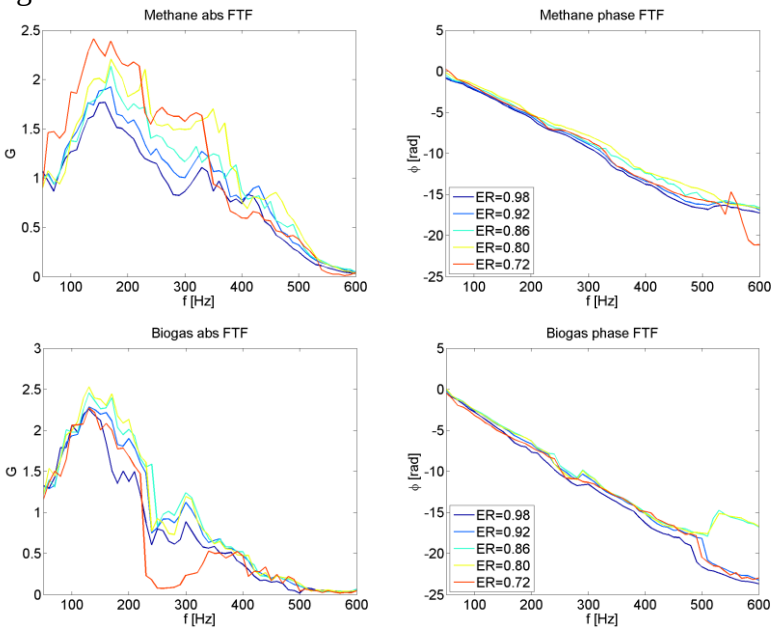

Figure 3. FTF magnitude and phase for methane (top) and biogas (bottom) varying ER

3.3 Limit cycle tests

Strong limit cycle conditions are naturally established with combustor lengths of both 1,250 and, in most of the cases, 900 mm. So, these two geometries were selected for these tests, where *Q'* and *p'* signals in the combustor were recorded, respectively, with PT0 and PMT (both, for 4 s at 4 kHz).

Experiments were carried out for the same fuels and ER as in FTF tests. With the 1,250 mm combustor, measurements were performed only with the inlet fully open, while all restriction settings listed above for the R_1 measurements were tested with the length of 900 mm. The experimental results and the comparison with predictions are discussed in the following section.

4. Results and discussions

4.1 Limit cycle results

Pressure amplitudes obtained with the burner of 1,250 mm for both CH_4 and biogas and different ER values can be observed in Fig. 4-a, while Fig. 4-b shows the frequency of the main peak in the pressure spectra (the frequency correspondence between *Q'* and *p'* has been verified for all tests).

Both fuels present high *p'* values, ranging from a minimum of about 200 Pa to a maximum of more than 2,500 Pa, with amplitude increasing as the mixture becomes leaner. CH_4 flames show higher pressure oscillations than biogas ones for all the ER tested, especially at lean conditions, where the difference is of about 4 times.

Methane flames present also higher oscillation frequencies than biogas, with values that increase almost linearly with ER. On the contrary, frequency results almost constant for biogas, with a slight change between ER=0.92 and 0.86.The changes in frequency are explained in part by the variation in flame temperature (and, so, in speed of sound), which gradually increases with ER and is higher for methane than for biogas. This effect, however, does not fully justify the variations observed for changes in fuel properties or fuel-air ratio. Most probably, the changes in FTF shown in Fig. 3 should also be accounted for, but this requires a more comprehensive analysis, combining both FTF and burner acoustics, for example using the dispersion equation, as shown below.

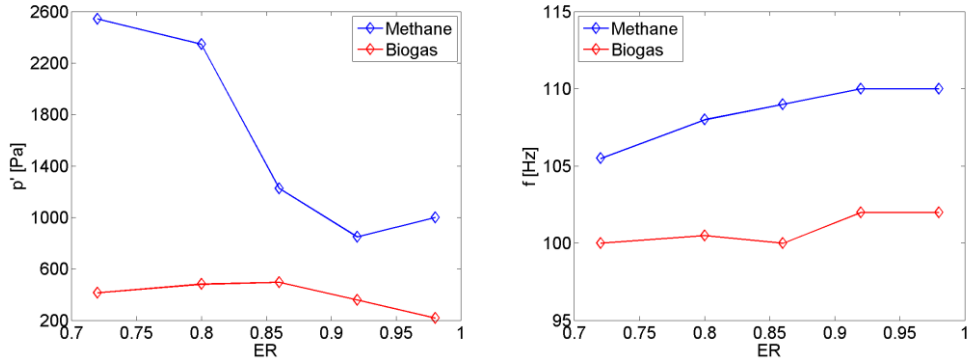

Figure 4. Amplitude and frequency of the main peak in *p'* spectra for methane and biogas. Combustor length=1,250 mm, *H*=-inf

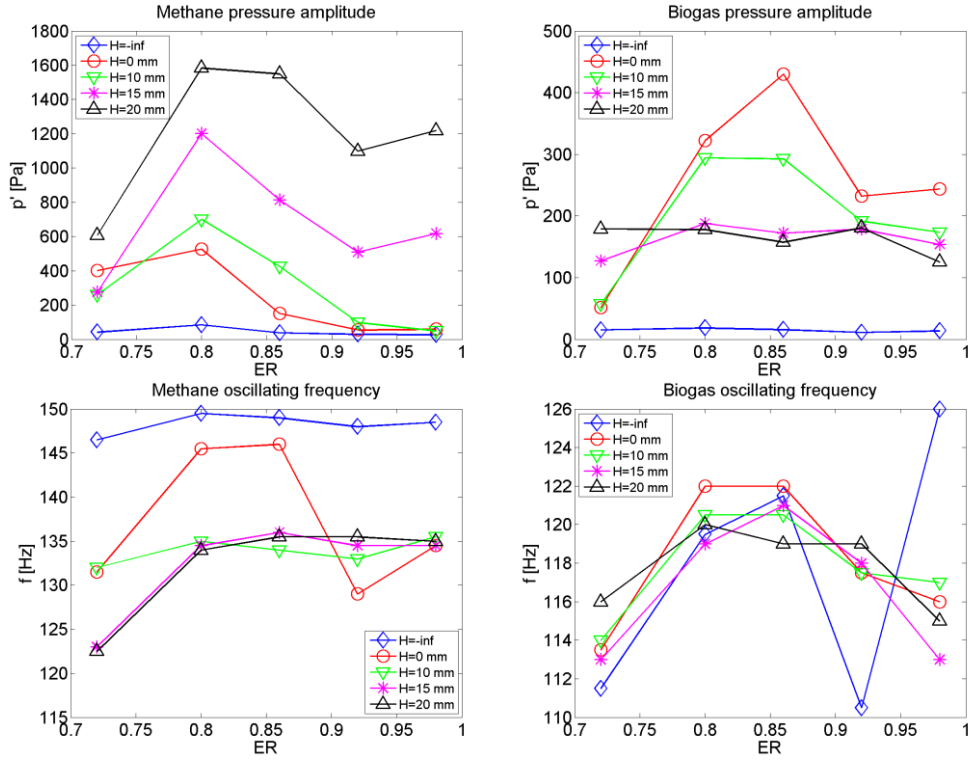

Figure 5. *p'* amplitude (top) and oscillation frequency (bottom) for methane (left) and biogas (right), for different upstream reflection coefficient. Combustor length=900 mm

Figure 5 shows *p'* amplitudes and frequencies obtained with the combustion chamber of 900 mm changing the upstream reflection coefficient. Methane shows very low *p'* amplitudes for an inlet completely open, while the instability tends to increase as the inlet is progressively closed (*H* increasing). The amplitude of the instability varies with the restriction level, but in all cases the strongest limit cycle occurs for ER=0.8.

Biogas, as methane, shows very low pressure fluctuations for fully open inlet (*H*=-inf), with instabilities triggered as the restriction is closed. However, in this case the dynamics does not increase monotonically with restriction level, but the most unstable case is represented by *H*=0 mm. Further increase in the inlet restriction causes a decrease in the combustion dynamics and only ER=0.72 suffers a slight increment of pressure fluctuation. Differently to methane, *p'* level is almost constant for any ER for the highest restriction tested (*H*=20 mm).

Biogas frequencies are almost the same for a given ER, irrespectively of the inlet restriction, while methane flames appear to shift between two characteristics frequencies, at 150 and 135 Hz approximately. The first mode is typical of a completely open inlet, whereas the second appears at high restriction levels. The intermediate condition with *H*=0 mm leads to an oscillating behaviour

between both modes depending on the ER value. Frequency values are less interpretable in terms of temperature in this case and are probably more conditioned by the reflection coefficient value and by the acoustic of the system.

4.2 Dispersion equation results

All tests presented in the previous section have been simulated using the dispersion equation. The solutions were identified as those yielding a result of approximately zero for Eq. (6). With that purpose, the angular frequency plane has been swept: from 50 to 600 Hz with 0.5 Hz steps for the real frequency and from -1000 to 1000 rad/s, with 1 rad/s steps, for the imaginary component.

The temperature inside the combustor is not known. Adiabatic temperature is not a good approximation, due to significant heat losses: the combustion chamber is cooled by 50 Nm^3/h of air flowing, in parallel and cocurrent with burnt gases, between the combustion chamber wall and an outer concentric shield, which in turn is refrigerated by a water jacket along its first 400 mm. Therefore, the temperature is significantly lower than the adiabatic one and, moreover, it varies noticeably along the axial distance (preliminary tests showed a temperature down to 400°C at the outlet for the 1,250 mm combustor). Since the dispersion equation requires a single temperature value for the whole combustion chamber, it was set at 50% of the adiabatic temperature (as calculated for different fuels and ER), as a reasonable approximation.

Another factor to be considered for a correct simulation is the burner length considered in the model: to represent a completely open outlet the combustor length must be artificially increased by $\delta=0.85\cdot D/2$, where D is the hydraulic diameter of the combustor [11, 12].

Due to space limitations, the analysis will be focused on the differences between experimental and predicted oscillation frequencies in order to assess the ability of this simple approach to identify the instability modes under limit cycle conditions. Figure 6-a and b present the difference between experimental frequencies (f_{ex}) and the modes predicted with the dispersion equation (f_{th}) for combustor lengths of 1,250 and 900 mm, respectively. Values of f_{th} have been chosen among the different solutions provided by the dispersion equation as the lowest frequency with a negative imaginary part. Overall, the differences obtained are below 10 Hz in 90% of the cases, with a maximum difference of 16 Hz.

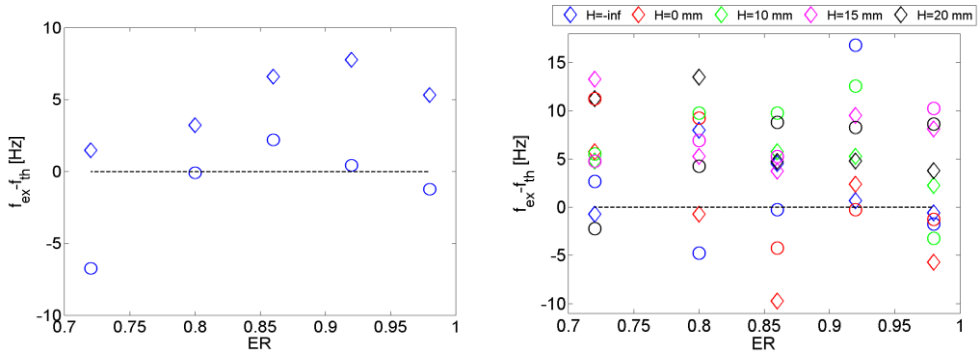

Figure 6. Differences between experimental and predicted frequencies; (◊) methane cases, (o) biogas cases. Left: burner of 1,250 mm, H=-inf. Right: burner of 900 mm for different inlet restriction settings

So, despite the simplifications involved, the use of linear FTF to simulate strong non-linear limit cycle conditions has shown to correctly predict unstable modes for a large variety of cases, including changes in conditions of very different nature (geometry, ER, fuel). A particular objective of this work was to test these methods against changes in the composition of the fuel, also with good results, in spite of the significant changes in flame properties for methane and for biogas. The description of the dynamic response of the flame in terms of the FTF measured for linear regimes seems to provide the information required to anticipate limit-cycle behaviour for different fuels.

The fact that the FTF gain does not describe the actual flame behaviour in non-linear conditions does not seem to lead to significant errors in the predictions of oscillation modes. The reason could

be that these results are mainly determined by the phase (rather than the gain) of the FTF, which barely changes from FTF to FDF, at least for the flame shape studied (V-flame). Nevertheless, further investigation would be required to verify this interpretation.

5. Conclusions

The FTF of two different fuels has been used as an input to a simplified network model to predict unstable modes for a wide range of operational conditions. The results obtained have been compared with experiments in which high pressure fluctuations are naturally obtained, reaching limit cycle conditions. Theoretical unstable modes obtained show a very good agreement with experimental frequencies, so indicating that the FTF contains the information required to predict instability modes, irrespectively of operational parameters. Apparently, the phase information contained in the FTF may be accurate enough (i.e., similar to the phase in non-linear conditions, as described by the FDF) to successfully identify the natural oscillation modes when the system reaches a limit cycle. Nevertheless, further work to confirm this conclusion is needed. The results presented are expected to complement the findings of previous works by extending the range of validation tests with a systematic study of different conditions, including biogas flames and their differences with respect to methane.

ACKNOWLEDGEMENTS

This work was supported by the Spanish Ministries of Science and Innovation, and of Industry and Competitiveness, through research projects CSD2010-00011 and 2016-4845, respectively.

REFERENCES

1 Dowling, A. and Stow, S. R. Acoustic Analysis of Gas Turbine Combustors, *Journal of Propulsion and Power*, **19** (5), 751-764, (2003)
2 Rayleigh, L. The explanation of certain acoustical phenomena, *Nature*, **18** 319-321, (1878)
3 Han, X., Li, J. and Morgans, A. S. Prediction of combustion instability limit cycle oscillations by combining flame describing function simulations with a thermoacoustic network model, *Combustion and Flame*, **162** (10), 3632-3647, (2015)
4 Noiray, N., Durox, D., Schuller, T. and Candel, S. A unified framework for nonlinear combustion instability analysis based on the flame describing function, *Journal of Fluid Mechanics*, **615** 139-167, (2008)
5 Palies, P., Durox, D., Schuller, T. and Candel, S. Nonlinear combustion instability analysis based on the flame describing function applied to turbulent premixed swirling flames, *Combustion and Flame*, **158** (10), 1980-1991, (2011)
6 Li, J. and Morgans, A. S. Time domain simulations of nonlinear thermoacoustic behaviour in a simple combustor using a wave-based approach, *Journal of Sound and Vibration*, **346** 345-360, (2015)
7 Kim, K. T., Lee, J. G., Quay, B. D. and Santavicca, D. A. Spatially distributed flame transfer functions for predicting combustion dynamics in lean premixed gas turbine combustors, *Combustion and Flame*, **157** (9), 1718-1730, (2010)
8 Kim, K. T. and Santavicca, D. Linear stability analysis of acoustically driven pressure oscillations in a lean premixed gas turbine combustor, *Journal of Mechanical Science and Technology*, **23** (12), 3436-3447, (2009)
9 Bellucci, V., Schuermans, B., Nowak, D., Flohr, P. and Paschereit, C. O. Thermoacoustic Modeling of a Gas Turbine Combustor Equipped With Acoustic Dampers, *Journal of Turbomachinery*, **127** (2), 372-379, (2005)
10 Noiray, N., Durox, D., Schuller, T. and Candel, S. Self-induced instabilities of premixed flames in a multiple injection configuration, *Combustion and Flame*, **145** (3), 435-446, (2006)
11 Lamraoui, A., Richecoeur, F., Ducruix, S. and Schuller, T. Experimental analysis of simultaneous non-harmonically related unstable modes in a swirled combustor *Proceedings of GT 2011*, Vancouver, Canada, (2011)
12 Richecoeur, F., Schuller, T., Lamraoui, A. and Ducruix, S. Analytical and experimental investigations of gas turbine model combustor acoustics operated at atmospheric pressure, *Comptes Rendus Mécanique*, **341** (1), 141-151, (2013)
13 Alemela, P. R., *Measurement and scaling of acoustic transfer matrices of premixed swirl flames*, Ph.D. Thesis, Technische Universität München, (2009)